Apr 26th - May 3rd

Axisymmetric Soil-Structure Interaction by Substructure Approach

P. K. Basu
Washington University, St. Louis, Missouri

B. J. Lee
Washington University, St. Louis, Missouri

Proceedings: First International Conference on Recent Advances in Geotechnical Earthquake Engineering and Soil Dynamics, April 26 - May 3, 1981, St. Louis, Missouri

AXISYMMETRIC SOIL-STRUCTURE INTERACTION BY SUBSTRUCTURE APPROACH

P.K. Basu, Associate Professor of Civil Engineering,
Washington University, St. Louis, Missouri

B.J. Lee, Research Assistant, Civil Engineering Dept.,
Washington University, St. Louis, Missouri

SYNOPSIS The effect of soil-structure interaction is incorporated into an existing finite element computer program for axisymmetric shells and plates using substructure approach and energy transmitting boundaries. The results of numerical experimentation for a tall chimney and a typical hyperboloidal cooling tower are presented.

INTRODUCTION

In the case of large scale structures like nuclear power plants, cooling towers, dams, etc., the importance of soil-structure interaction in seismic analysis has been recognized. The availability of powerful numerical tools coupled with virtually unlimited power of present day digital computers have heightened the expectations of both design engineers and regulating agencies, in this area. This has resulted in increased efforts to tackle the problem of soil-structure interaction in an accurate but practical manner.

In a particular situation, the importance of soil-structure interaction depends upon the relative stiffness of the subgrade and the supported structure. For instance, in the case of structures supported on a soft soil, the response of the structure may be significantly modified due to the flexibility of the subgrade and energy dissipation in subgrade by hysteretic action and radiation.

A number of analytical and numerical approaches [1-6] have been put forward to tackle the problem. As analytical methods are applicable to idealized situations only, the use of numerical methods like the finite element method [5-8], which can easily handle many practical situations, have become popular. The approaches followed by different workers differ from each other depending upon the way the semi-infinite nature of the subgrade, the input earthquake motion, the flexibility of the footing, the constitutive properties of the soil, and the effect of embeddment of the structure are treated [6].

In order to save computational effort and be able to treat directly the specified free-field motion at the base of the structure as the excitation, the substructure method is preferred over the, so called, direct method where the combined structure-subgrade system is considered simultaneously. A very efficient way to restrict the horizontal dimensions of the subgrade to reasonable limits is to define a, so called, energy transmitting boundary at the edge of the footing to account for the loss of energy due to the radiation of waves outside the core-region [5, 8]. Although such a definition does not allow embeddment [8] and requires a rigid stratum within a reasonable depth, recent developments seem to have removed this restriction [9].

Although most of the numerical developments in the area of soil-structure interaction has been restricted to plane strain condition, considerable work [2,7,10], both analytical and numerical, has been carried out in the case of axisymmetric problems using rigid circular footings. The subgrade has universally been treated as either purely elastic or visco-elastic.

The main objectives of this paper are first, to discuss the approach used to implement the soil-structure interaction capability in an existing finite element analysis program (SHORE-III) [11] for axisymmetric shells and plates, and secondly, to present and discuss some results of numerical experimentation using the resulting modified program (to be called SHORE-IV) [12] in the case of a tall concrete chimney and a hyperboloidal cooling tower, both under seismic excitation.

ASSUMPTIONS

1. The subgrade is elastic and layered.
2. The vertical extent of the soil is restricted by an impervious stratum.
3. To simulate the semi-infinite extent of the subgrade, a cylindrical energy transmitting boundary of the type used by Kausel and Rosset [7] is assumed to exist at the circumferential perimeter of the footing.
4. The structure is supported on flexible ring footing which is treated as a rotational shell element so that radial strain is assumed zero and the strains along circumferential and meridional directions are assumed to vary linearly.
5. The embeddment of the structure is small
6. The seismic free-field motion acts at the base of the structure.
7. Internal damping in the subgrade is proportional.
8. All the phenomenon of soil-structure interaction can be described by means of complex stiffness (impedance) functions established at the structure-soil interface.
9. For radiation damping, the imaginary part of the complex stiffness matrix is used.

FINITE ELEMENT MODEL OF SUBGRADE

Just as in the superstructure, a cylindrical coordinate system (r, θ,z) is used to define a point in the subgrade as shown in Fig. 1. The displacement components are expressed in terms of Fourier series in θ as

$$\begin{aligned} u &= u_j \cos j\theta \\ u &= u_j \sin j\theta \\ w &= w_j \cos j\theta \end{aligned} \tag{1}$$

Likewise, the loading is also expressed in terms of Fourier series. The strain-displacement and constitutive relationships are expressed as

$$\begin{aligned} \{\bar{\epsilon}\} &= [A]\{\bar{u}\} \\ \{\bar{\sigma}\} &= [D]\{\bar{\epsilon}\} \end{aligned} \tag{2}$$

in which

$\{\bar{\epsilon}\}$ = the strain vector

= $\{\bar{\epsilon}_{rr}, \bar{\epsilon}_{zz}, \bar{\epsilon}_{\theta\theta}, \bar{\gamma}_{zr}, \bar{\gamma}_{r\theta}, \bar{\gamma}_{\theta z}\}$ and,

$\{D\}$ = the constitutive matrix in terms of Lame's constants.

The dynamic equilibrium equation of the subgrade can be expressed in the form

$$[H]\{Z\} = 0 \tag{3}$$

in which

$$[H] = \begin{bmatrix} \frac{2H_j}{\partial r} & 0 & \frac{j}{r}H_j \\ & k H_j & \\ \text{Symm.} & & \frac{\partial H_j}{\partial r} \end{bmatrix}, \text{ and}$$

$$\{Z\} = \begin{Bmatrix} k(\lambda+2G)(f_2'-kf_1) + G(f_1''-kf_2') + \rho\Omega^2 f_1 \\ (\lambda+2G)(f_2''-kf_1') + \mu k(f_1'-kf_2) + \rho\Omega^2 f_2 \\ G(f_3''-k^2 f_3) + \rho\Omega^2 f_3 \end{Bmatrix}$$

With H_j = Hankel function of the second kind for j^{th} harmonic;

k = wave number

f_1, f_2, f_3 = function of Z, k, Ω (driving frequency) and the velocities of shear and compression waves.

The core region of the subgrade, i.e. the region enclosed by the energy transmitting boundary, is discretized by well known quadratic isoparametric ring elements of quadrilateral cross-section, Fig. 2. The equilibrium equation of the core region can be expressed in the form

$$(K - \Omega^2 M)U = P \tag{4}$$

in which

K = core stiffness matrix

P = load vector for the core region

U = displacement vector for the core region

The motion at the interface of the core and outer region (i.e. for field) should be conforming. Accordingly, the above equation will be modified by the dynamic stiffness functions relating the interface stresses with corresponding displacements. Such a relationship can be obtained [7] from the principle of vertical displacement by defining a discrete eigenvalue problem for the outer region in which the expansion for displacements in Z-direction are assumed to be of same form as used for the finite elements of the core region. The interface displacements in the far field can then be expressed in terms of eigenfunctions corresponding to the natural modes of wave propagation in the subgrade leading to a quadratic eigenvalue problem

$$(Ak^2 + Bk + C)\bar{U} = 0 \tag{5}$$

in k and a boundary load vector

$$P_b = R_b U_b \tag{6}$$

where R_b is a function of [A], [D], the wave member k, etc. For further details see Refs. [7] and [12] From Eqs. (4) and (6) after suitably expanding R_b,

$$[K]_s\{U\} = \{P\} \tag{7}$$

in which

$$[K]_s = [K] - \Omega^2[M] + [R]$$

EQUIVALENT BOUNDARY SYSTEM

The modified equilibrium Eq. (7) is partitioned into terms corresponding to the surface nodes appearing over the width of the ring foundation, i.e. u_f, and those corresponding to the rest of the core region, i.e. u_r Using standard condensation techniques the terms corresponding u_r are removed to obtain an equivalent stiffness matrix corresponding to u_f. The resulting reduced stiffness matrix will be complex and, of course, be a function of Ω. The real and imaginary parts of the stiffness matrix can be separated and will respectively represent the stiffness and damping (due to radiation) effects of the subgrade. These effects corresponding to the three interface nodes can be replaced by a set of axial and rotational springs located at the interface of the ring footing and subgrade. Since the ring footing is modeled by the same rotational shell element as is used in the superstructure, it is necessary to locate the equivalent springs in the center of the footing corresponding to the degrees of freedom shown in Fig. 3. The interface stiffness matrix can then be expressed as

$$[k_f] = [T][k_s] \tag{8}$$

in which

$[k_f]$ = the stiffness matrix for the equivalent system
= $[k_u, k_v, k_w, k_{\beta\varphi}, k_{\beta\theta}]$

$[k_s]$ = the interface stiffness matrix corresponding to the three nodes at the interface

$[T]$ = the transformation matrix

$$= \begin{bmatrix} 0 & 0 & 1 & 0 & 0 & 1 & 0 & 0 & 1 \\ 0 & 1 & 0 & 0 & 1 & 0 & 0 & 1 & 0 \\ 1 & 0 & 0 & 1 & 0 & 0 & 1 & 0 & 0 \\ 0 & 0 & 0 & 0 & 0 & B^2/4 & 0 & 0 & B^2/4 \\ 0 & 0 & 0 & 0 & B^2/4 & 0 & 0 & B^2/4 & 0 \end{bmatrix}$$

EXAMPLES

In order to check the effectiveness of the energy transmitting boundary, a series of parametric studies were carried out [13] with the subgrade model of SHORE-IV by varying the mesh size, stratum depth, and driving frequency. From parametric studies with stratum depth it was found that in the case of a very deep stratum, the lower boundary can be assumed at a depth equal to three times the outer radius of the footing (r_o). From studies on mesh size it was found that up to a depth of 1.5 r_o it is necessary to ensure that the longest element dimensions is not greater than one-sixth the shear wave length. Moreover, whenever the ratio r_o/B is large the width of the ring elements can be progressively increased towards the axis of symmetry. It was also found that both translational and rotational stiffnesses of the subgrade are sensitive to changes in driving frequency. However, the damping elements were found to be less dependent on the driving frequency.

In order to study the effect of soil-structure interaction on some practical axisymmetric shell structures, two examples, see Figs. 2 and 11, are considered.

Response Spectrum Analysis of a Tall Chimney: The chimney of Fig. 2 was analyzed using the horizontal response spectrum shown in Fig. 4. A damping ratio of 5% was used. The properties of the materials of the subgrade were assumed as follows.

Layer	G (MN/m^2)	ν	ρ ($kN\text{-}sec^2/m^4$)
Top	25	0.4	1.8
Middle	28	0.35	1.9
Bottom	30	0.33	1.8

The subgrade was modeled with 16 isoparametric quadratic ring elements and analyzed with a driving frequency equal to the fundamental frequency of the chimney on rigid foundation. In order to determine the effect of relative stiffnesses of shell and subgrade the modulus of elasticity of the chimney was varied (12430 to 24850 MN/m^2) and thus relatively stiff and flexible subgrade conditions were realized. The chimney was modeled with 22 high-precision rotational shell elements. The fundamental frequency of the chimney was found to drop from 1.69 rad/sec. (flexible chimney) and 2.39 rad/sec. (stiff chimney) for rigid base condition to 1.45 rad/sec. and 1.85 rad/sec. when soil-structure interaction was considered. Reanalysis of the subgrade with different values of driving frequencies between the above limits did not seem to affect the responses of the full system appreciably. The stress resultants N_φ, N_θ, and M_φ for rigid base and flexible base conditions are shown in Figs. 5 to 7. It may be noted that the discrepancy between fixed and flexible base conditions is localized mostly near the stiffener level with smaller values being indicated for flexible base, i.e. when soil-structure interaction is included. On the other hand, in the results presented in Figs. 8 to 10 for relatively flexible subgrade, the discrepancy between flexible and fixed base conditions are more pronounced. Also, near the upper part of the chimney, the flexible base condition gives notably higher N_φ than the stiff base condition.

Time History Analysis of a Hyperboloidal Shell: The cooling tower shown in Fig. 11 was analyzed with 5 seconds of El-Centro (5,18, 1940) EW Comp. earthquake record. A damping ratio of 5% was assumed and numerical integration in the time domain was carried out using Newmark-β method. Analysis was performed for both flexible base condition with a time step of 0.005 sec. Following the recommendations of Pandya and Setlur [14] two kinds of subgrade were considered

(i) a 15m deep layer of uniform medium sand with a relative density of 75%, overlying solid rock. The values of G and ν were taken as 88 MN/m^2 and 0.35 respectively, and

(ii) a 18m deep layer of stiff clay overlying solid rock. The values of G and ν were taken as 111.1 MN/m^2 and 0.3 respectively.

In order to arrive at the equivalent boundary system (EBS), the subgrade was analyzed with a driving frequency of 12.34 rad/sec., which is the fundamental frequency for the shell with rigid base. The fundamental frequencies for the two subgrades including the effect of the superstructure was found to be 11.84 and 12.02 rad/sec , which represent discrepancies of less than 5%. The results of time history analysis for both rigid and flexible base conditions are shown in Figs. 12 & 13. It may be noted that the predominant force components, i.e. N_φ near the base and N_θ at top, are not significantly affected by the flexible base condition. Similar agreements were noted in the case of displacements and moments. It may, however, be cautioned that the response may change significantly if more realistic foundation elements like piles or cassions are used.

CONCLUSIONS

The parametric studies exhibited that the energy transmitting boundary gives a reasonable approximation to the far field effect. For discretizing the subgrade only a few suitably proportioned quadratic isoparametric elements are necessary. The concepts of transmitting boundary and substructuring are very efficient ways to reduce the computational effort in the soil-structure interaction analysis of axisymmetric structures. SHORE-IV can be used for the efficient soil-structure interaction analysis of those axisymmetric shell and plate structures for which the stated assumptions regarding the subgrade and footing are valid. From the limited numerical experimentation with a typical chimney and a cooling tower with idealized support conditions,

the importance of soil-structure interaction in the case of some axisymmetric shell structures is recognized. Although, in the case of the cooling tower problem the effect of soil-structure interaction does not seem to be significant, definite conclusions in this regard can only be drawn after further numerical experimentation with more realistic foundation conditions.

REFERENCES

1. Whitman, R. V., and F. E. Richart, Jr., (1967), "Design Procedures for Dynamically Loaded Foundations", Jl. of Soil Mech. and Foundation Div., Proc. ASCE, Vol. 93, SM6, pp. 169-193.

2. Richart, F. E., Jr., J. R. Hall, Jr., and R. D. Woods (1970), "Vibration of Soil and Foundations", Prentice-Hall, Inc.

3. Lysmer, J., and R. L. Kuhlemeyer (1969), "Finite Dynamic Model for Infinite Media", Jl. of Engrg. Mech. Div., Proc. ASCE, Vol. 95, EM4, pp. 859-877.

4. Roesset, J. M., R. V. Whitman and R. Dobry (1973), "Modal Analysis of Structures With Foundation Interaction", Jl. of St. Div., Proc. ASCE, Vol. 99, ST3, pp. 399-416.

5. Kausel, E., J. M. Rosset and G. Waas (1975), "Dynamic Analysis of Footings With Layered Media", Jl. of Engrg. Mech. Div., Proc. ASCE, Vol. 101, EM5, pp. 679-693.

6. "Analysis for Soil-Structure Interaction Effects for Nuclear Power Plants", Report by the Ad Hoc Group on Soil Structure Interaction of the Committee on Nuclear Structures and Materials of the Structures Division of ASCE, 1979.

7. Kausel, E. and J. M. Rosset (1975), "Dynamic Stiffness of Circular Foundations", Jl. of Engrg. Mech. Div., Proc. ASCE, Vol. 101, EM6, pp. 771-785.

8. Gutierrez, J. A. (1976), "A Substructure Method for Earthquake Analysis of Structure-Soil Interaction", Report No. EERC 76-9, University of California, Berkeley.

9. Dasgupta, G. (1980), "Foundation Impedance Matrices by Substructure Deletion", Jl. of Engrg. Mech. Div., Proc. ASCE, Vol. 106, EM3, pp. 517-523.

10. Luco, J. E. and R. A. Westmann (1971), "Dynamic Response of Circular Footings", Jl. of Engrg. Mech. Div., Proc. ASCE, Vol. 7, EM5, pp. 1381-1395.

11. Basu, P. K. and P. L. Gould (1977), "SHORE-III, Shell of Revolution Finite Element Program - Theoretical Manual and Users Manual", Research Report Nos. 48 and 49, Structural Division, Washington University, St. Louis.

12. El-Shafee, O. M., P. K. Basu and P. L. Gould (1980), "SHORE-IV, Finite Element Program for Dynamic and Static Analysis of Shells of Revolution - Theoretical and Users Manual", Research Report Nos. 57 and 58, Structural Division, Washington University, St. Louis.

13. El-Shafee, O. M. (1979), "Dynamic Analysis of Shells of Revolution - Soil Systems", Doctoral Dissertation, Washington University, St. Louis.

14. Pandya, V. and A. Y. Setlur (1975), "Seismic Soil-Structure Interaction by Finite Elements: Case Studies", Proc. of Second ASCE Specialty Conf. on Structural Design of Nuclear Plant Facilities, Vol. 1-A, pp. 826-848.

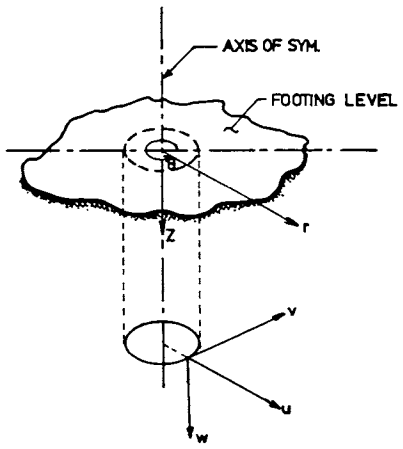

Figure 1. Coordinate System for the Subgrade

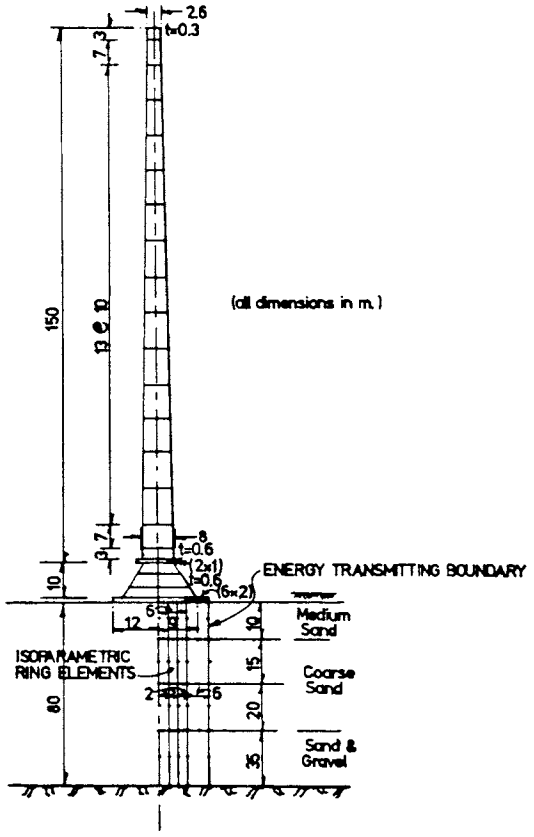

Figure 2. Concrete Chimney on an Elastic Subgrade

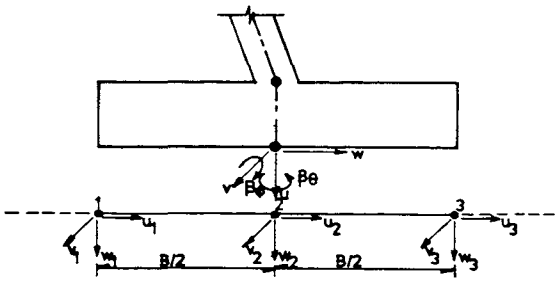

Figure 3. Degrees of Freedom at Footing Subgrade Interface

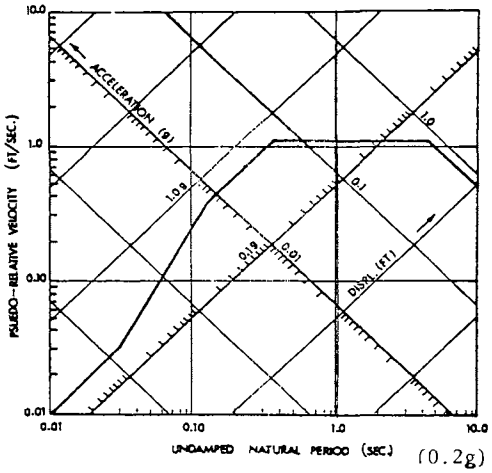

Figure 4. Horizontal Response Spectrum (0.2g)

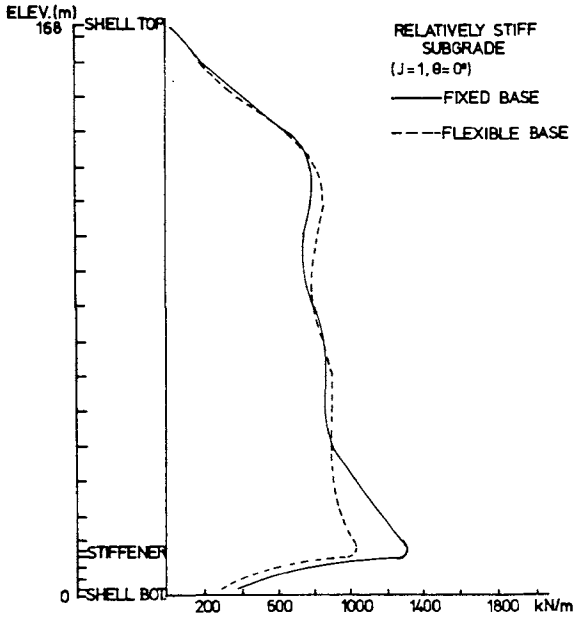

Figure 5. Variation of Membrane Force N_ϕ in Chimney

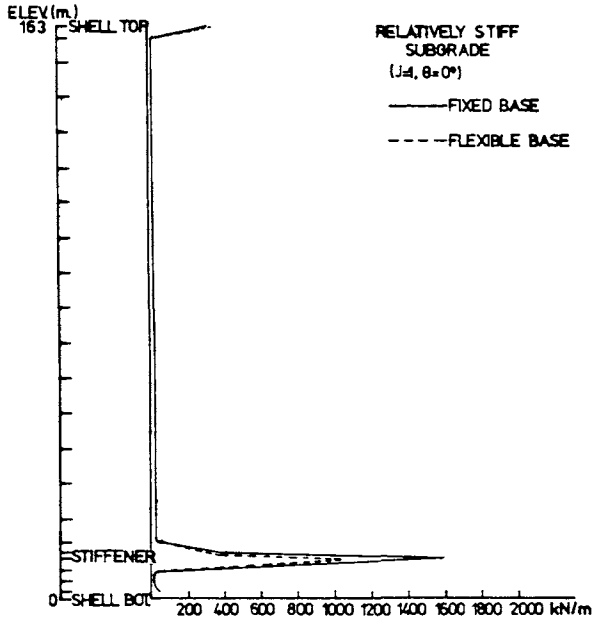

Figure 6 Variation of Membrane Force N_θ in Chimney

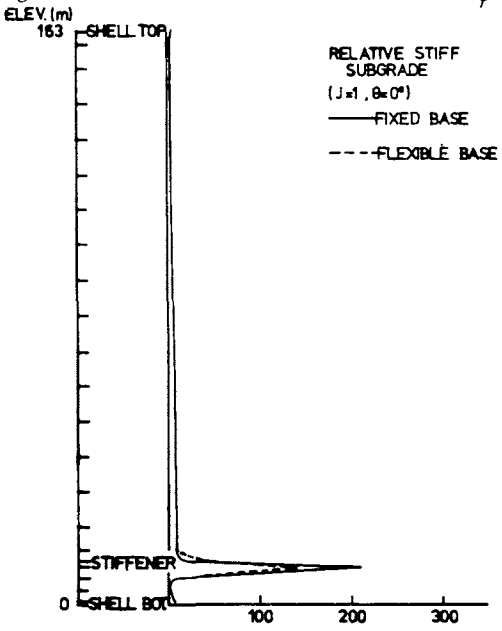

Figure 7. Variation of Moment M_ϕ in Chimney

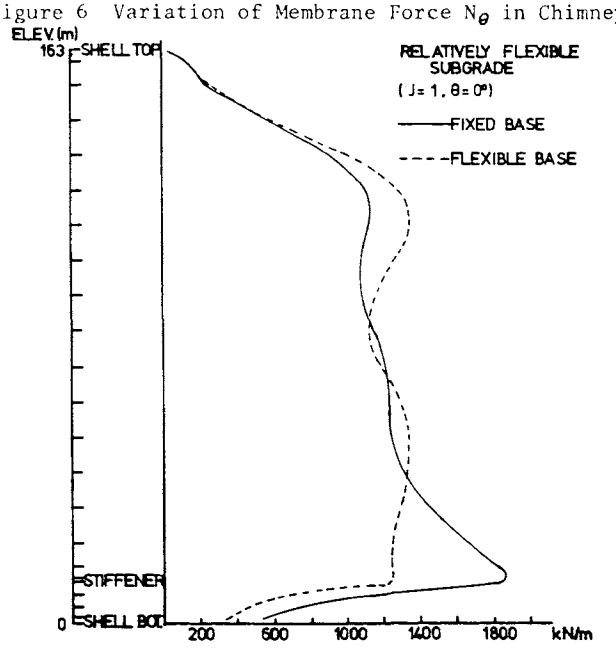

Figure 8 Variation of Membrane Force N_ϕ in Chimney

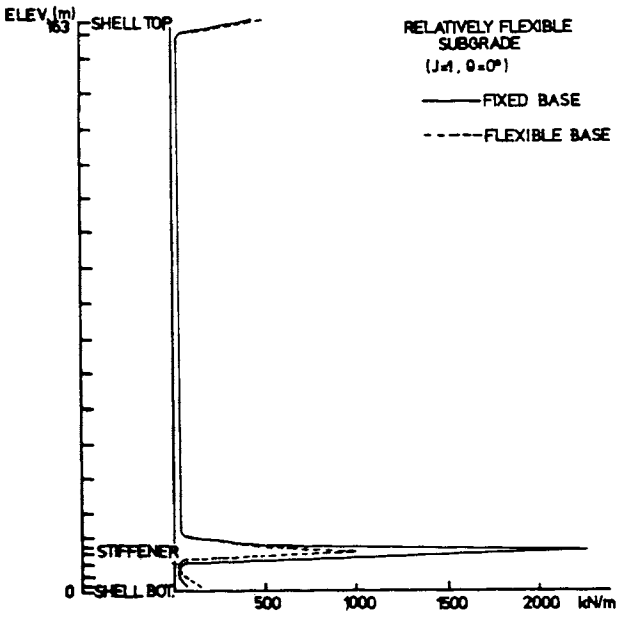

Figure 9. Variation of Membrane Force N_θ in Chimney

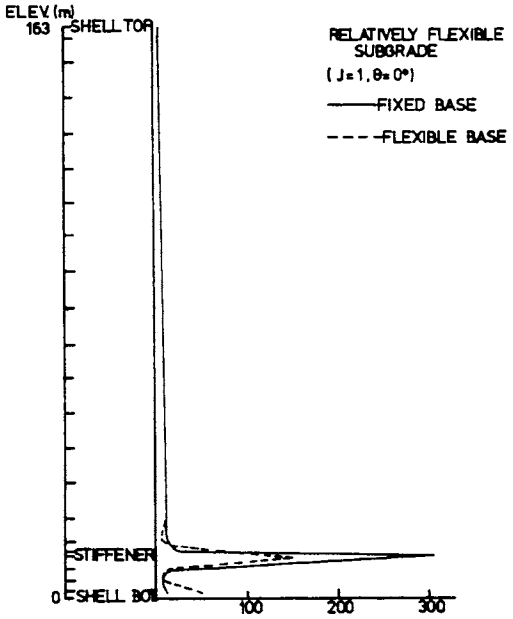

Figure 10. Variation of Moment M_ϕ in Chimney

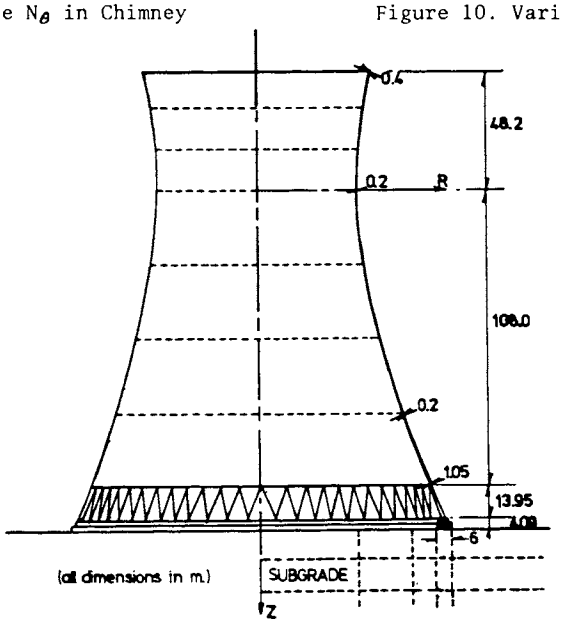

Figure 11. Hyperboloidal Cooling Tower on Elastic Subgrade

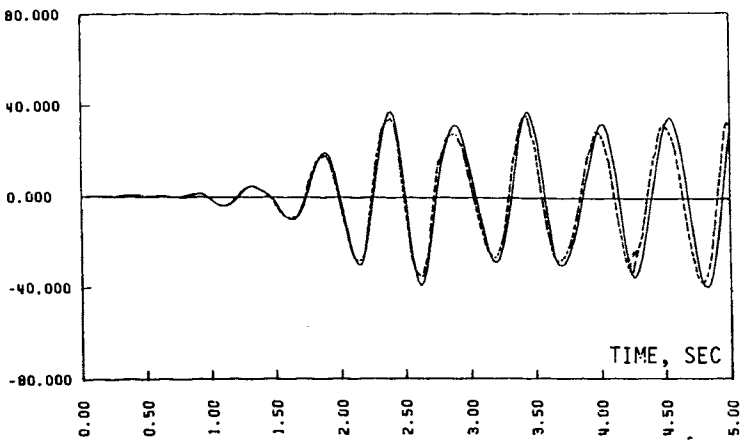

Figure 12. Time History Plot for N_ϕ at Seventh Node From Top

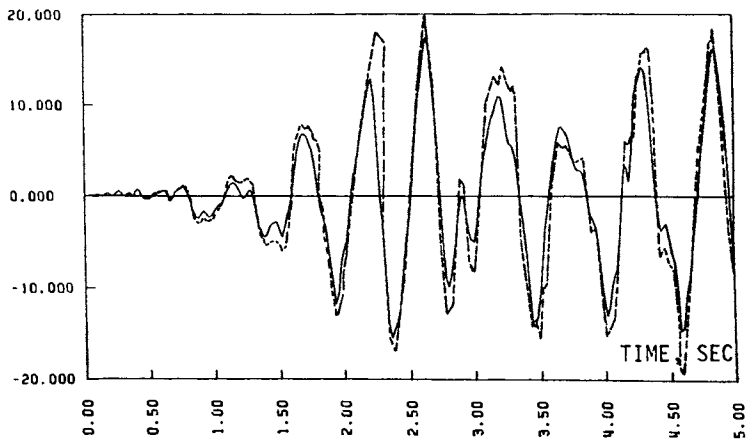

Figure 13 Time History Plot for N_θ at Top